Image Cover Sheet

CLASSIFICATION	SYSTEM NUMBER 511910
UNCLASSIFIED	

TITLE

The Characterisation of Piezoelectric and Electrostrictive Materials for Underwater Acoustic Transducers

System Number:

Patron Number:

Requester:

Notes: Paper #36 contained in Parent sysnum #511874

DSIS Use only:

Deliver to: CL

THE CHARACTERISATION OF PIEZOELECTRIC AND ELECTROSTRICTIVE MATERIALS FOR UNDERWATER ACOUSTIC TRANSDUCERS

Binu K. Mukherjee, Stewart Sherrit and Guomao Yang

Department of Physics, Royal Military College of Canada,
Kingston, Ontario, Canada K7K 7B4.
[e-mail: mukherjee@rmc.ca ; tel: 613 541 6000 x 6348]

ABSTRACT

Underwater acoustic transducers are used extensively in Anti-Submarine Warfare and Mines Countermeasures. The majority of these transducers are based on the use of piezoelectric and electrostrictive materials as the active material in the transducer. These materials are also important for the active methods of sound absorption that are being considered for underwater stealth. Since the materials are non-linear and lossy, the design of the various devices requires a good and precise knowledge of the dielectric, elastic and piezoelectric/electrostrictive properties of the materials under the actual conditions of the particular application (e.g. high power, pre-stress, etc..,). The importance of such a precise knowledge of the properties has increased with the development of software, such as PZFlex, which can model piezoelectric materials/transducers and their vibrations very accurately if precise material parameters are provided. The Laboratory for Ferroelectric Materials at the Royal Military College of Canada has, over the last few years, developed a range of experimental methods for determining the full matrix of the dielectric, elastic and piezoelectric/electrostrictive properties of piezoelectric and electrostrictive materials as complex coefficients, to take account of all types of losses in the material, and to determine the coefficients as a function of temperature, frequency and applied fields, stresses and hydrostatic pressures. We review these methods and discuss the kind of detailed information on material parameters that can now be made available to transducer designers.

INTRODUCTION

Piezoelectric and electrostrictive materials are important constituents of electromechanical sensors, actuators and smart structures. Piezoelectric materials produce a strain, S, under the influence of an external electric field, E, or become electrically polarised under the influence of an external stress, T. The property of piezoelectricity is closely related to the phenomenon of ferroelectricity, which describes the spontaneous polarisation in a crystal that can be changed between two or more distinct directions with respect to the crystal axes through the

application of an external electric field. This ability of ferroelectric materials to switch polarisation under an external electric field from a random orientation to a preferred direction is used in a variety of polycrystalline ferroelectric materials (ceramics and polymers) to produce a polycrystalline piezoelectric material with a net preferred polarisation direction. This process is described by the term "poling". Prior to poling, individual domains of the ceramic are piezoelectric but the random orientations counteract each other and the net effect is that the macroscopic material shows little or no piezoelectricity. The partial alignment of the domains during poling creates a net spontaneous polarisation in the poling direction and the material shows a C_∞ symmetry around that direction.

Piezoelectricity can be mathematically described by a phenomenological model derived from thermodynamic potentials. The derivations are not unique and the set of equations describing the direct and converse piezoelectric effect depend on the choice of potential and the independent variables used[1,2]. For example, one such set of linear constitutive relations is:

$$S_p = s^E_{pq} T_q + d_{pm} E_m$$
$$D_m = \varepsilon^T_{mn} E_n + d_{pm} T_p \qquad (1)$$

where D is the electric displacement, s is the elastic compliance, d is a piezoelectric constant and ε is the dielectric permittivity. The superscripts of the constants designate the independent variable that is held constant when defining the material coefficient and the subscripts define tensor directions which take into account the anisotropic nature of the material. The elements of the tensor form a 9x9 matrix with 1,2,3 designating the orthonormal directions (3 is the poling direction) and 4,5,6 designating the shear directions. For the commonly used polycrystalline piezoelectric ceramic materials with C_∞ symmetry, such as lead zirconate titanate or PZT, there are ten non-zero, independent matrix elements consisting of 5 independent elastic constants, 3 independent piezoelectric constants and 2 independent dielectric constants. For these materials, the reduced matrix form of the above constitutive relationships can now be written as:

$$\begin{bmatrix} S_1 \\ S_2 \\ S_3 \\ S_4 \\ S_5 \\ S_6 \\ D_1 \\ D_2 \\ D_3 \end{bmatrix} = \begin{bmatrix} s^E_{11} & s^E_{12} & s^E_{13} & 0 & 0 & 0 & 0 & 0 & d_{13} \\ s^E_{12} & s^E_{11} & s^E_{13} & 0 & 0 & 0 & 0 & 0 & d_{13} \\ s^E_{13} & s^E_{13} & s^E_{33} & 0 & 0 & 0 & 0 & 0 & d_{33} \\ 0 & 0 & 0 & s^E_{55} & 0 & 0 & 0 & d_{15} & 0 \\ 0 & 0 & 0 & 0 & s^E_{55} & 0 & d_{15} & 0 & 0 \\ 0 & 0 & 0 & 0 & 0 & 2(s^E_{11} - s^E_{12}) & 0 & 0 & 0 \\ 0 & 0 & 0 & 0 & d_{15} & 0 & \varepsilon^T_{11} & 0 & 0 \\ 0 & 0 & 0 & d_{15} & 0 & 0 & 0 & \varepsilon^T_{11} & 0 \\ d_{13} & d_{13} & d_{33} & 0 & 0 & 0 & 0 & 0 & \varepsilon^T_{33} \end{bmatrix} \begin{bmatrix} T_1 \\ T_2 \\ T_3 \\ T_4 \\ T_5 \\ T_6 \\ E_1 \\ E_2 \\ E_3 \end{bmatrix} \qquad (2)$$

While the linear constitutive relations can be written in ways other than shown in (1), there are only 10 independent constants and the IEEE Standard on Piezoelectricity[3] contains the appropriate equations that allow one to convert from one set of equations/matrix to another. Ideally, under small fields and stresses and for materials with low losses within a limited frequency range, these 10 constants contain all the information required to predict the behaviour of the material when a stress, strain or electric field is applied to it. However, piezoelectric materials generally exhibit varying degrees of non-linearity. If the above linear equations are used to define the material constants of piezoelectric materials, then the material constants themselves are a function of applied fields and stresses as well as of the temperature of the material. Also, the piezoelectric response is not instantaneous and the response time can be important in some applications.

The most general way to take account of the dielectric, mechanical and piezoelectric losses in a material is to express the 10 material constants as complex coefficients. This paper first reviews the experimental methods for determining these complex material constants for any piezoelectric material and the effects of dispersion on these constants, and it discusses the use of an appropriate equivalent circuit for the material to include all types of losses. The paper then reviews the experimental methods to study the non-linear dependence of the material constants on applied signals as well as the response time of the materials.

RESONANCE METHODS FOR DETERMINING THE COMPLEX MATERIAL CONSTANTS

The most widely used technique for determining the material constants for piezoelectric materials is the resonance technique as outlined in the IEEE Standard on Piezoelectricity[3]. A piezoelectric sample of specific geometry is excited with an AC signal and an impedance analyser is used to determine the complex impedance and admittance as a function of frequency. Typical spectra are shown in Figure 1 and it can be seen that the spectra contain resonances that result from ultrasonic standing waves in the material. Several particular frequencies may be defined from the spectra: the parallel resonance frequency f_p is the frequency at which the resistance R is a maximum; the sideband frequencies $f_{+1/2}$ and $f_{-1/2}$ correspond to the maximum and the minimum in the reactance X; The series resonance frequency f_s is the frequency at which the conductance G is a maximum; and, the sideband frequencies $f_{+1/2s}$ and $f_{-1/2s}$ correspond to maximum and the minimum of the susceptance B.

The five most common modes used for piezoelectric ceramic analysis are shown in Figure 2 along with the recommended geometrical aspect ratios for samples used to determine each mode. The arrow marked on each sample indicates the poling direction for the piezoelectric ceramics. The aspect ratios ensure that the sample is excited in a mode where the one-dimensional approximation is valid and that coupling between the modes is negligible. In some materials (typically low mechanical Q materials) these aspect ratios may be relaxed

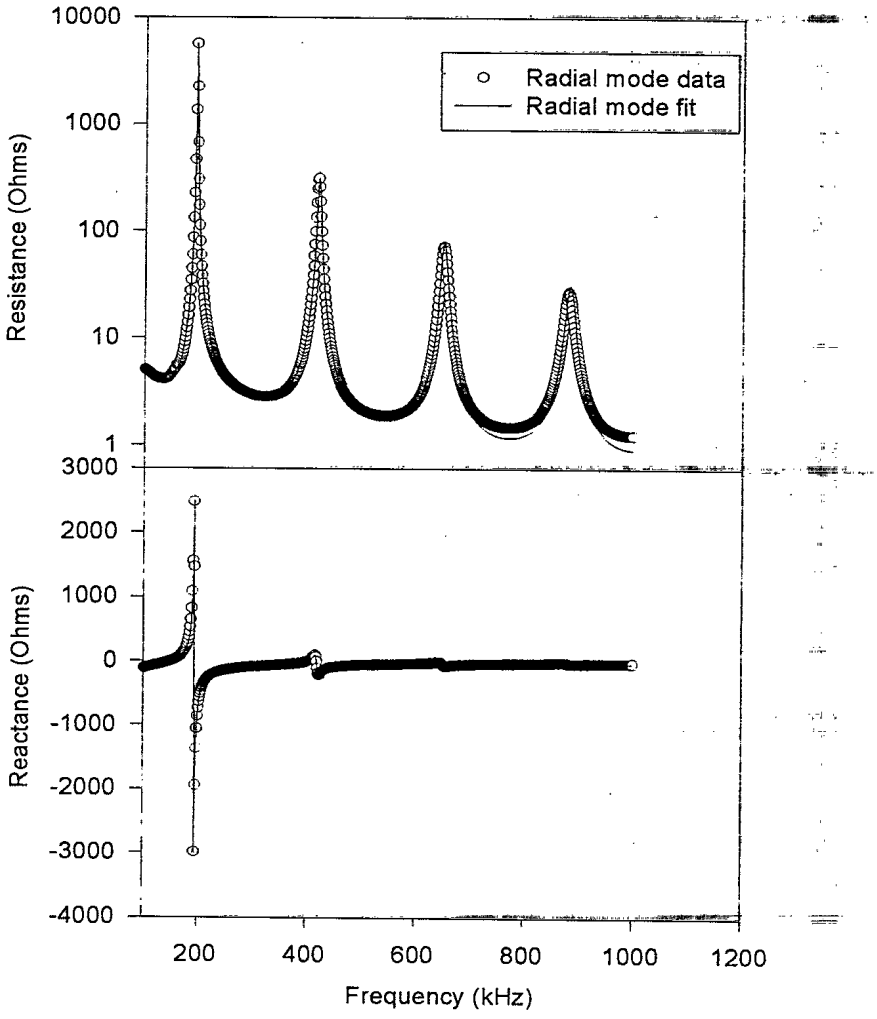

Figure 1. The impedance spectra for the radial mode of a Motorola 3203 HD PZT disk sample.

whereas in other materials (high Q and high electromechanical coupling) they may need to more stringent.

The impedance equations that govern the various resonance spectra have been derived from the phenomenological theory of piezoelectricity[4,5] for the case of real material constants assuming lossless materials. These equations express the impedance as a function of the appropriate material constants and of the particular frequencies defined above. Holland[6] showed that the losses in a piezoelectric material may be taken into account by representing the material constants as complex coefficients. Sherrit[7] has re-derived the expressions for the impedance for the various resonance geometries using complex material constants so as to include the dielectric, mechanical and piezoelectric losses in the material.

The IEEE Standard on Piezoelectricity uses the impedance equations for lossless resonators and the critical frequencies derived from the equations to determine the real parts of the material constants. Numerous techniques have been proposed to measure the material constants as complex coefficients[8,9,10,11,12,13,14]. Basically, the expression for the impedance is compared with the experimental curve around resonance and the material constants are found so as to obtain the best fit.

As an example, Figure 3 shows the impedance plots for the thickness extensional resonance for Motorola PZT 3203 HD ceramic. For this case the linear piezoelectric equations are

$$T_3 = c_{33}^D S_3 - h_{33} D_3 \quad \text{and} \quad E_3 = -h_{33} S_3 + \frac{1}{\varepsilon_{33}^E} D \tag{3}$$

where h is the piezoelectric constant and c is the elastic stiffness. Considering the material constants to be complex, these equations can be used to derive the expression for the impedance for the thickness extensional resonance:

$$Z = \frac{l}{i\omega A \varepsilon_{33}^S}\left(1 - \frac{k_t^2 \tan\left(\frac{\omega}{4f_p}\right)}{\frac{\omega}{4f_p}}\right), \tag{4}$$

where the electromechanical coupling constant k_t and the parallel resonance frequency f_p are given by

$$k_t^2 = \frac{\varepsilon_{33}^S h_{33}^2}{c_{33}^D} \qquad 2f_p = \frac{1}{l}\sqrt{\frac{c_{33}^D}{\rho}}$$

Radial Mode
(20t<D)

Thickness Mode
for Plate
($10t < w_1$ $10t < w_2$)
also disk with (20t<D)

Length Extensional
($l > 5w_1$, $l > 5w_2$)
also rod with (l > 5D)
these are minimum aspect ratio

Thickness Shear Mode
(w_1 and $w_2 > 10t$)

Length Thickness Mode
(l >10t, and w >3t, l >3w)

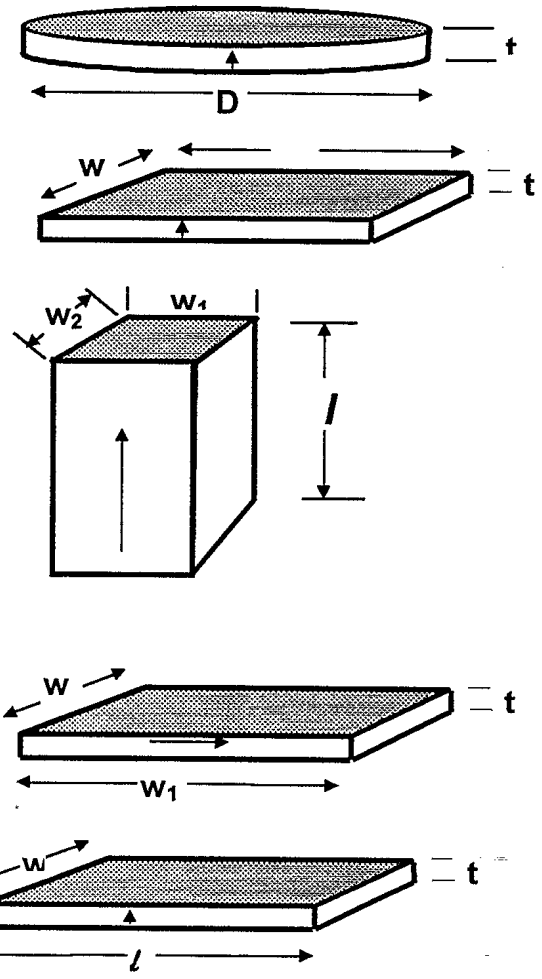

Figure 2. The geometry and poling direction for the five most common modes of piezoelectric resonators for materials characterisation. Note: The radial mode also has a thickness resonance and the length extensional resonator may also be of the form of a long rod.

The material constants around the fundamental resonance can be found by fitting expression (4) to the resonance curves shown in Figure 3. This is done by using Smits' method[11] which uses impedance values at three frequencies of which one is chosen near the frequency at which the resistance is a maximum and the other two are chosen to be above and below the resonance. Two of the points plus an initial guess for the elastic constant, using a relationship between the mechanical Q and the resonance bandwidth described by Land et al[15], are used to calculate electromechanical coupling constant and the permittivity. Using the coupling constant and a third point, a new elastic constant is calculated and the process is repeated until convergence. A disadvantage of Smits' technique is that impedance values can vary by several orders of magnitude around resonance and so care must be taken that the measuring

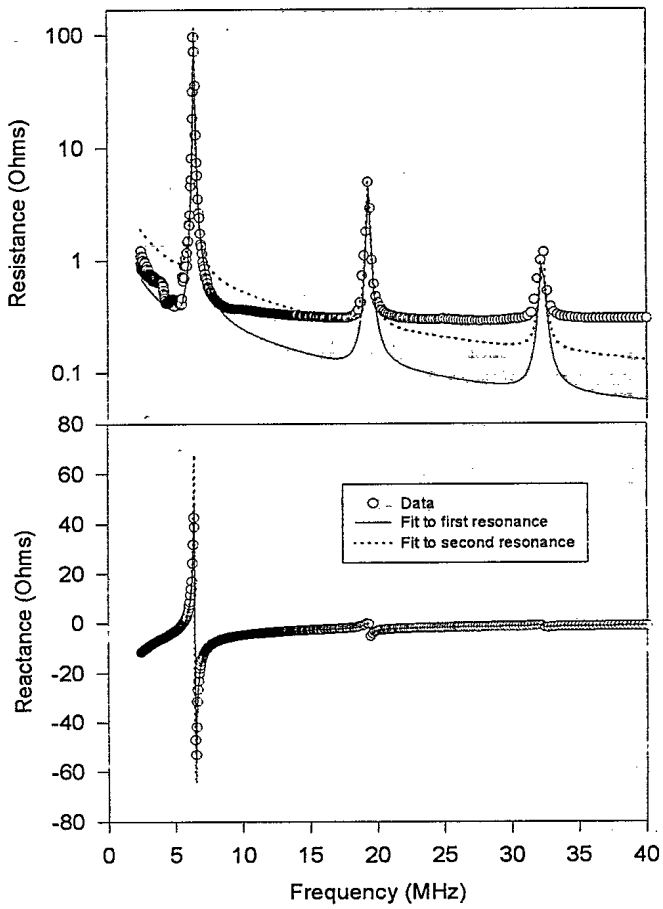

Figure 3. The resistance and reactance data of the thickness extensional resonance and the fit to the first and second resonance peaks for Motorola 3203HD ceramic. The resistance is plotted on a logarithmic scale.

instrument is not overloaded and that the impedance values are carefully determined. The values of the material constants will depend to some extent on the points chosen to analyse the spectrum but this dependence can be corrected by repeating the analysis with a different choice of points followed by an averaging of the results. Alemany et al[14] have looked at procedures to obtain convergence during iterations. A non-iterative technique to determine the material constants has been presented by Sherrit et al[12]. This technique requires frequency data around resonance and impedance data away from resonance. Although the disadvantage associated with Smits' method is removed, this method is less accurate when dispersion in the material constants is significant. Smits' technique can be used to find the material constants that determine the thickness, thickness shear, length and length thickness modes of resonance. The complex material constants for the radial extensional resonance can be found using a method put forward by Sherrit et al[13]. A commercial software is now available for carrying out the analysis of the resonance curves[16]. By analysing all the different modes of resonance the complete set of material constants can be determined around the resonance considered. An example of such a determination for the Motorola 3203 HD PZT ceramic is shown in Table 1[17].

DISPERSION

The effects of dispersion can be studied by determining the material constants at the fundamental frequency of resonance and at higher resonances. Figure 3 shows that the fit obtained by using the material constants around the fundamental frequency does not agree well with the impedance curve around the second resonance and vice versa. This method has been used to study dispersion in the Motorola 3203 HD ceramic by Sherrit et al[17]. Thus, the material constants can be determined for frequencies required by the applications engineer as long as a reasonable resonance curve can be experimentally determined near the required frequencies. In some cases it is possible to express the real and imaginary parts of the material constant as a polynomial in frequency, as shown by Sherrit et al for piezoelectric polyvinylidene difluoride – tetrafluoroethylene (PVDF-TrFE) copolymer[18]; the applications engineer can use the polynomials to find the material constants at a desired frequency.

EQUIVALENT CIRCUIT

In designing devices it is sometimes useful to have an equivalent electrical circuit to represent the material. Currently the most widely used equivalent circuit to represent a piezoelectric vibrator in the thickness mode is the Van Dyke circuit, which is shown in Figure 4(a). This circuit uses four real circuit parameters, C_0, C_1, L_1 and R_1 to represent the impedance of a free-standing piezoelectric resonator around resonance. However the impedance, expressed by equation (4), contains six material constants (the real and imaginary parts of the permittivity,

Table 1: The reduced matrix of Motorola 3203HD PZT including the electromechanical coupling determined at the fundamental resonance of each mode.

Material Constant	Model	Frequency (kHz)	Value		% Standard Deviation	
			Real	Imag	Real	Imag
s_{11}^E (m^2/N) x10^{-11}	LTE	71.5	1.56	-0.030	0.63	5.2
s_{11}^E (m^2/N) x10^{-11}	RAD	150.9	1.55	-0.032	0.45	2.8
s_{11}^E (m^2/N) x10^{-11}	Average		1.56	-0.031		
s_{12}^E (m^2/N) x10^{-11}	RAD	150.9	-0.420	0.012	3.90	4.9
s_{13}^E (m^2/N) x10^{-11}	Calculated	Smits' formula	-0.821	0.034	N/A	N/A
s_{13}^E (m^2/N) x10^{-11}	Calculated	Matrix inversion	-0.825	0.017	N/A	N/A
s_{33}^E (m^2/N) x10^{-11}	LE	199	1.89	-0.034	1.0	0.78
s_{55}^E (m^2/N) x10^{-11}	TS	2730	3.92	-0.13	2.9	4.3
s_{66}^E (m^2/N) x10^{-11}	Calculated	IEEE formula	3.96	-0.086	N/A	N/A
c_{33}^D (N/m^2) x10^{11}	TE	6390	1.77	0.023	2.0	11
d_{13} (C/N) x10^{-12}	LTE	71.5	-297	9.7	0.70	7.1
d_{13} (C/N) x10^{-12}	RAD	150.9	-293	10	0.68	5.8
d_{13} (C/N) x10^{-12}	Average		-295	9.9		
d_{33} (C/N) x10^{-12}	LE	199	564	-15	3.1	17
d_{15} (C/N) x10^{-12}	TS	2730	560	-30	4.6	11
ε_{11}^T (F/m) x10^{-8}	TS	2730	2.14	-0.13	0.44	6.8
ε_{33}^T (F/m) x10^{-8}	RAD	150.9	3.06	-0.11	1.1	6.5
ε_{33}^T (F/m) x10^{-8}	LT	71.5	2.83	-0.061	1.9	9.4
ε_{33}^T (F/m) x10^{-8}	Average		2.95	-0.083		
ε_{33}^S (F/m) x10^{-8}	TE	6390	1.06	-0.053	2.0	4.2
k_{33}	LE	199	0.763	-0.0029	0.52	45
k_{13}	LTE	71.5	0.447	-0.0054	0.90	16
k_{15}	TS	2730	0.611	-0.0034	3.1	37
k_P	RAD	150.9	0.706	-0.0062	0.45	6.1
k_t	TE	6390	0.536	-0.0050	0.46	12

the coupling constant and the elastic stiffness) and therefore six parameters are needed to describe the impedance when losses are significant. We have proposed an

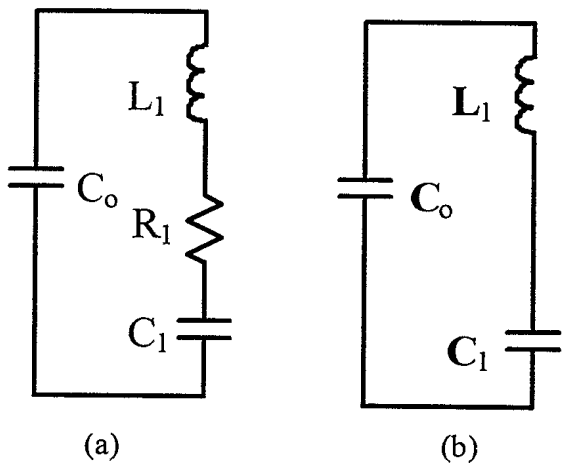

Figure 4. (a) The Van Dyke circuit model; the values of the circuit elements are real. (b) The proposed circuit model; the values of the circuit elements are complex.

alternative circuit model based on the lossless resonator model suggested by Butterworth[19] and Cady[20] and shown in Figure 4(b). The model contains three circuit elements C_0, C_1 and L_1 and we modify the model by assuming that each of these circuit elements be considered to be complex. The circuit now has six parameters and some unique features that make it an ideal model for representing the electrical characteristics of an unloaded piezoelectric resonator. We have shown[21] how the values of the complex circuit elements can be calculated from the complex material constants and vice versa and that spectra obtained by using the complex circuit model give very good agreement with corresponding experimental spectra for high Q as well as low Q materials.

QUASISTATIC EXPERIMENTS

The set of equations (1) is used to interpret most quasistatic measurements. Two experimental conditions may be used to simplify the measurement. If the stress is set to zero (i.e. the sample is free to expand unhindered), the equations are no longer coupled and the strain and the electric displacement can be measured as a function of the electric field. Similarly, if the electric field is zero (the short circuit condition), the strain and the dielectric displacement can be measured as a function of the stress. These uncoupled relationships are shown in Table 2.

Table 2. The quasistatic measurements that can be made in the 33 direction (along the poling axis) on a piezoelectric material with one of the independent variables set to zero.

Boundary Condition	Simultaneous Equations	
T = 0 (unclamped) Apply E - measure S and D	$S = dE$	$D = \varepsilon^T E$
E = 0 (short circuit) Apply T - measure S and D	$S = s^E T$	$D = dT$

MEASUREMENT OF THE PIEZOELEECTRIC CONSTANT AND THE PERMITTIVITY AS A FUNCTION OF THE APPLIED ELECTRIC FIELD

The variation of the piezoelectric constant d and the permittivity ε as a function of the applied electric field can be carried out under two different experimental situations: (a) quasistatic experiments, which gives the value of the constants under near DC conditions, and (b) resonance experiments, which yield the material constants at the appropriate resonance frequency. The difference in the significance of these two types of measurement can be understood with reference to Figure 5. The main curve in the figure shows a typical curve that is obtained when a varying electric field, below the coercive field, is applied to a piezoelectric material and the resultant strain is measured. A measurable hysteresis is found and this is due to the reversible and irreversible domain wall motions that are characteristic of ferroelectric materials. Under a large electric field the domain walls move to maintain a minimum in the domain energy and some of the domains engulf other domains or change shape irreversibly, which contributes to the net strain and polarisation. The onset of irreversibility in such materials has been studied by Zhang et al[22] who found that each material has a plateau region where the permittivity and the piezoelectric constant were independent of field and they attributed this field independence to reversible domain motion. In the case of resonance measurements, the AC measurement signal is small, well below the plateau region found by Zhang et al, and so the measurements correspond to reversible domain motions. Such AC resonance measurements have been carried out with an applied DC bias field to determine the variation of the material constants as a function of the DC field. The illustrative diagram in Figure 5 shows clearly that the slopes of the two types of measurement are different and therefore the material constants found from the two types of measurements cannot be the same. This discussion underlines the importance of determining the material constants under conditions appropriate for any particular application.

The quasistatic measurements were carried out with an optical lever experiment[23] that allows the strains in the 1 or 3 directions to be determined directly as a function of an applied dc field in the 3 direction whose maximum value exceeds the reversibility limit. The dielectric displacement was measured at the same time. Results[24] for the case of Motorola PZT 3203HD ceramic are shown in Figure 6 and they exhibit the typical hysteresis behaviour of ferroelectric materials. The shapes of the curves depend on the size and the change in the electric field.

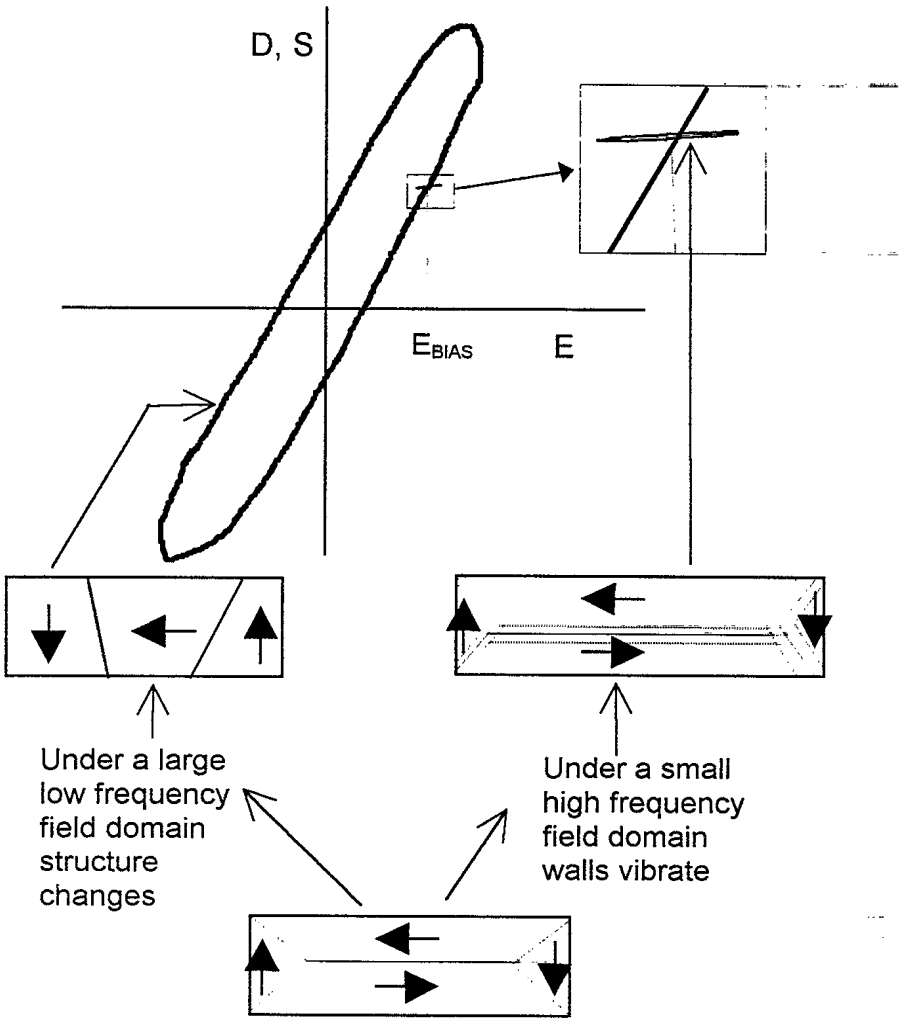

Figure 5. The relationship between the reversible and irreversible domain motion and the resultant strainor electric displacement as a function of the electric field.

If the maximum applied field is kept below the coercive field (0.5 to 1.0 MV/m for the Motorola ceramic), the non-linearities and the hysteresis are much less significant as can be seen in the curves in Figure 7. The figures show curves (loops) for six different maximum applied fields in each case and it can be seen that the slope and the hysteresis increase as the maximum field of the loop is increased. Since the hysteresis is now less significant, an average slope can be used to determine the material constants. The piezoelectric constants and the permittivity are plotted as a function of the maximum applied field in Figure 8. Although these constants represent average values, they would be useful, for example, to an actuator designer who is mainly interested in the strain level as a function of the applied field. The piezoelectric charge coefficients and the permittivity are found to vary linearly as a function of the applied electric field. These variations can be expressed as follows:

$$S = d_{33}E + q_{33}E^2 \quad \text{and} \quad D = \varepsilon_{33}E + (\kappa_{33}/2)E^2, \qquad (5)$$

where q_{33} is the electrostrictive coefficient and κ_{33} is the second order dielectric constant which we call the electrodielectric constant. It should be noted that κ_{33} represents the contribution which is caused by the coupling of the polarisation to the electric field.

The non-linear properties of the piezoelectric materials have also been studied by carrying out AC resonance measurements under DC bias[24] but, as explained above, the material constants obtained by these measurements correspond to reversible domain motions and are different from those obtained from the quasistatic measurements. The difference is illustrated in Table 3 which gives the values of the electrostrictive and electrodielectric coefficients obtained from the two types of measurements.

As pointed out above, the non-linearities are much less significant if the applied fields are below the coercive field so that a greater range of linear behaviour can be found with materials with higher coercive fields. For example, the piezoelectric polymer PVDF-TrFE has properties[25] that are relatively independent of the applied electric field for fields up to ± 0.4 MV/m; however this copolymer exhibits a much greater dispersion than does the ceramic PZT. This shows that the device designer needs to choose his material carefully depending on the performance requirements of the device.

STRESS AND TEMPERATURE DEPENDENCE OF THE DIRECT PIEZOELECTRIC CHARGE COEFFICIENT

The relationship between the dielectric displacement D and the stress T has also been studied[26]; this corresponds to the second experimental condition shown in Table 2 and the results show how the piezoelectric d constant varies as a function of the applied stress and the temperature of the specimen. The experimental arrangement has been described earlier[7,27]; the sample is compressed by a stress T and the resulting piezoelectric current is measured by a low input impedance electrometer operating in the current mode. The sample temperature can be set by a heat lamp and it can be measured by means of a thermocouple.

Table 3: The electrostriction and electrodielectric constants determined from the quasi-static and DC biased resonance spectra.

Non linear Coefficient Real Part	Quasi-static Maximum E_{DC}=0.39MV/m f < mHz	Length thickness Resonator E_{DC}=0.39MV/m f =72 kHz	Length Resonator E_{DC}=0.016MV/m f =572 kHz
κ_3 (Fm/V)	7.3×10^{-14}	1.8×10^{-14}	1.4×10^{-14}
q_3 (m^2/V^2)	9.5×10^{-16}	N/A	1.4×10^{-16}
q_1 (m^2/V^2)	3.1×10^{-16}	5.0×10^{-17}	N/A

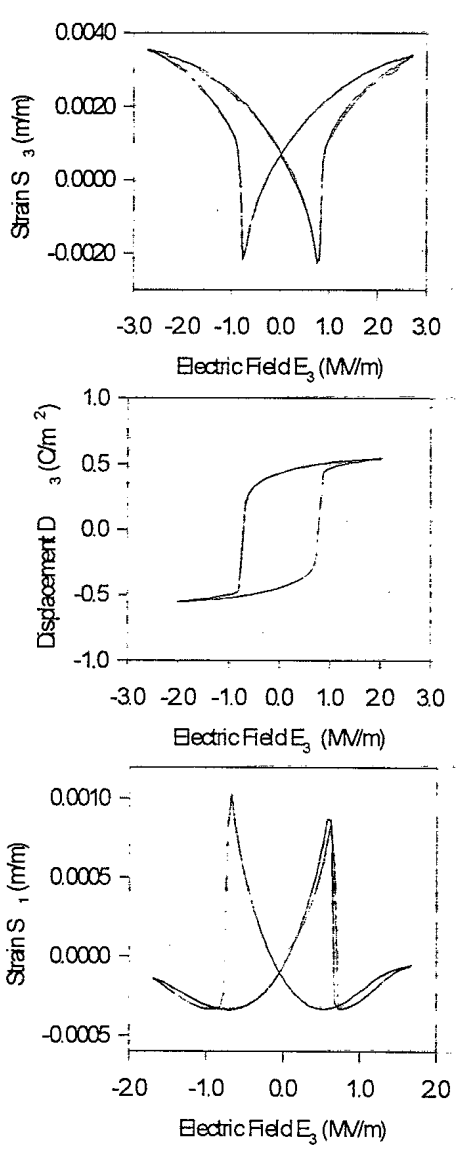

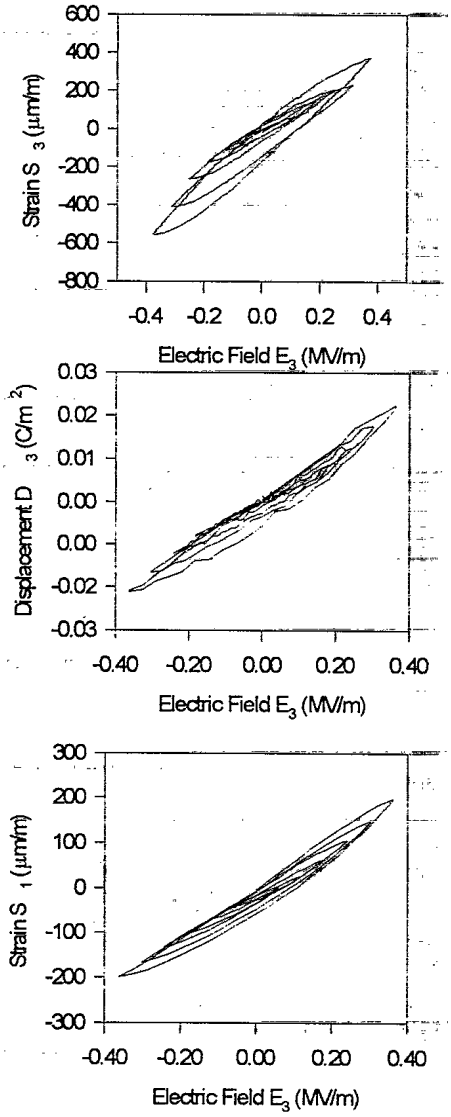

Figure 6. The quasistatic field dependence of the strain S_3, the dielectric displacement D_3 and the strain S_1 as a function of electric field to field levels above the coercive field.

Figure 7. The quasistatic field dependence of the strain S_3, the electric displacement D_3 and the strain S_1 as a function of field to field levels below the coercive field. In each case six loops with different maximum fields are shown.

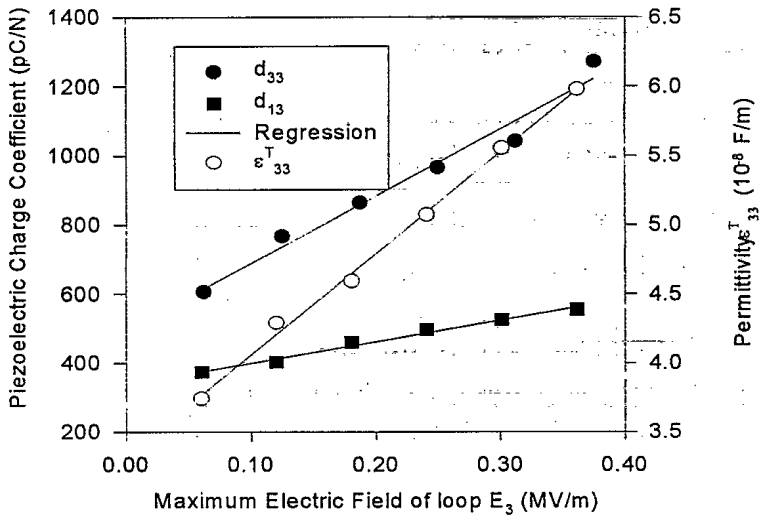

Figure 8. The quasistatic field dependence of the effective piezoelectric constant and permittivity as a function of the field up to field levels below the coercive field. The slopes give the higher order material coefficients.

The application of a steadily increasing stress generates a polarisation that produces a current, I, through the electrometer. If the stress is increased as a function of time, t, the current produced is directly proportional to the piezoelectric charge coefficient and the relationship is given by

$$D_3 = \frac{1}{A}\int I\partial t = d_{33}T_3 \qquad (6)$$

where A is the electroded area of the sample. The technique can determine an integrated average value of the charge coefficient up to the stress level T_3, as defined by

$$d_{33}(T_3) = \frac{\int I\partial t}{AT_3} \qquad (7)$$

Sherrit et al[7] have used this technique to measure the charge coefficient, d_{33}, for a Channel 5804 PZT ceramic as a function of the applied stress and the temperature and their results are shown in Figure 9. At room temperature, the application of a stress of around 70 MPa increases the value of d_{33} by a factor of about two, once again emphasising the importance of the non-linear effects. The shape of the d_{33} curves as a function of stress appears to flatten and become more linear as the temperature is increased.

THE PIEZOELECTRIC RESPONSE TIME

The curves shown in Figure 9 were measured under increasing stress and hysteresis was observed when the stress was ramped down. This suggested that the results would depend on the ramp rate of the stress and that time dependent effects were involved. In order to study the response time, Sherrit et al[26,27] applied a step stress with a rise time of less than 10 seconds and measured the current as a function of time elapsed after the application of the stress. The step stress resulted in a step increase in the current and, most interestingly, the current then decayed over a period of time, almost exactly following the inverse relationship I = k/t. Any mechanical relaxation in the experimental system or any relaxation in the in the elastic constant would only have resulted in a negative current. Sherrit et al were therefore able to attribute the continued current to the continued generation of charges in the specimen which is likely to result from slow changes to the domain structure in the specimen, particularly the 90° reorientation of domains, which require atomic motion and are therefore expected to be slower than the 180° reorientation of domains that require only a shift in the charge centre of the domain. When a step stress is applied, there is a near instantaneous generation of charge due to 180° domain changes and some 90° domain changes and this is followed by the slow switching of other 90° domains that gives rise to the observed continued generation of charge and slow decay in the current. Both the fast and the slow domain changes contribute to the piezoelectric charge coefficient and, using equation (7), this can now be expressed as

$$d_{33} = d_{33}^{0} + d_{33}^{t}\, ln(t) = d_{33}^{0} + \frac{\int \frac{k}{t}\partial t}{AT_3}, \qquad (8)$$

where $d_{33}^{t} = k/AT_3$ is a constant that describes the time dependence of the current as well as that of d_{33}.

From the point of view of applications, it is important to note that the observed time dependence results in a frequency dependence for the piezoelectric charge coefficient. A high frequency signal will produce a charge that, to a first order, is proportional to d_{33}^{0}, while a low frequency will produce a charge that has contributions from both d_{33}^{0} and d_{33}^{t}.

Figure 10 shows the variation of the charge coefficient, d_{33}, for the Channel PZT 5804 PZT ceramic as a function of the temperature and the time after the imposition of the stress signal. The slope of the curves, which determines d_{33}^{t}, is seen to increase with increasing temperature and Sherrit et al[26,27] were able to obtain a roughly linear Arrhenius plot of $\ln(d_{33}^{t} T)$ as a function of inverse temperature, $1/T$, corresponding to the expression

$$d_{33}^{t} = \frac{d_{33}^{t0}}{T} exp\left(\frac{-E_a}{KT}\right), \qquad (9)$$

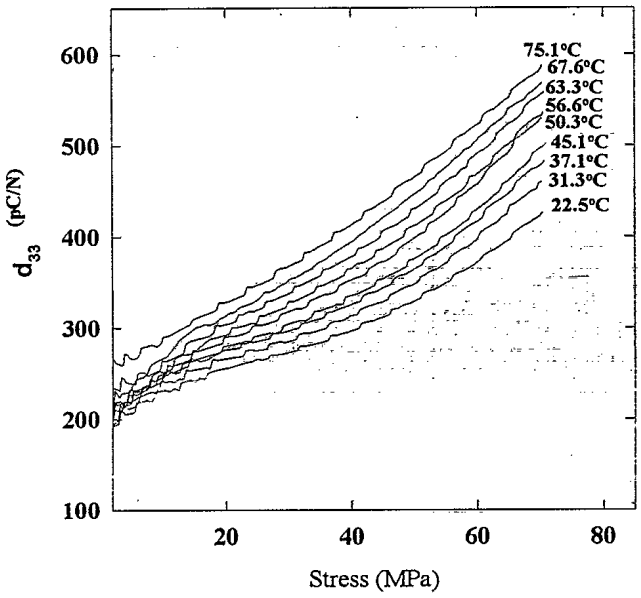

Figure 9. The value of d_{33} as a function of stress and temperature for a Channel 5804 PZT ceramic.

where E_a is an average activation energy for domain motion, d_{33}^{t0} is a pre-exponential factor and K is Boltzmann's constant. They found an average activation energy of 0.39 eV for the Channel 5804 PZT and their measurements on a variety of PZT types yielded activation energies in the range from about 0.2 eV to 0.7 eV. The time dependence coefficient d_{33}^{t} was found to be independent of the stress level while the coefficient k, which describes the time dependence of the current due to the generation of charge, was found to be linearly dependent on the stress T_3 up to 60 MPa..

FUTURE WORK

We are currently setting up to carry out the resonance measurements with the specimen in a thermally controlled temperature. This will enable us to determine the full matrix of material coefficients as a function of temperature.

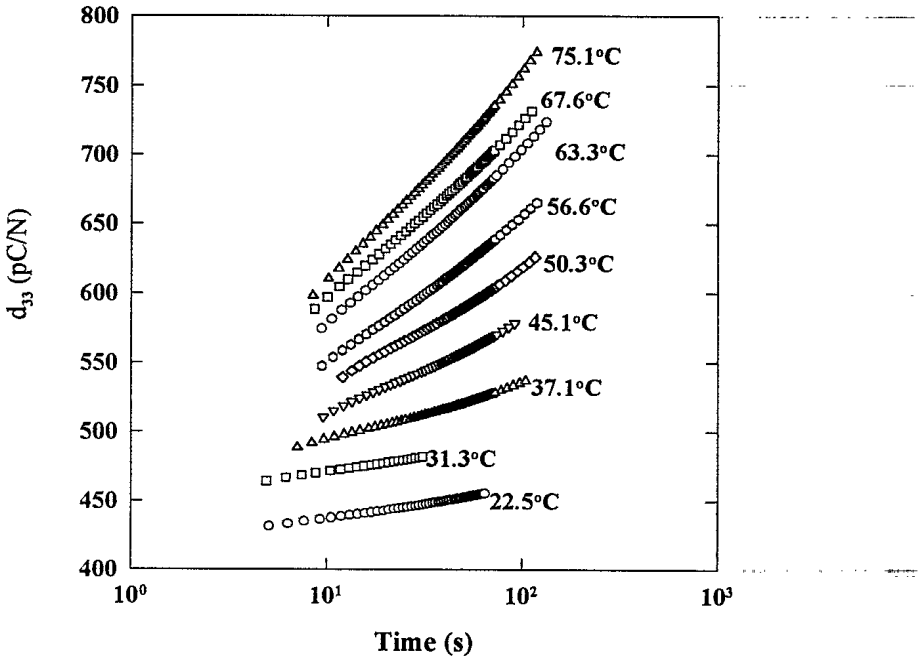

Figure 10. The value of d_{33} as a function of the time after the application of a stress step.

CONCLUSIONS

The experimental results reviewed in this paper clearly show that piezoelectric materials have significant non-linear effects. It follows that the material constants measured under the application of small signals, which are the parameters usually provided by the manufacturers, are not sufficient to predict the behaviour of the materials when large signals are applied, as, for example, in actuators and acoustic projectors. The device designer requires material constants that are measured under the conditions which prevail during the operation of the device, and this paper has reviewed some of the experiments that are available to make such measurements.

ACKNOWLEDGEMENT

We gratefully acknowledge funding support from the Defence Research Establishment Atlantic and the Academic Research Programme of the Department of National Defence, Canada as well as support from the Office of Naval Research, USA given through the Naval Undersea Warfare Centre, Newport, RI, USA.

REFERENCES

[1] A.F. Devonshire, *Phil. Mag. Supp.*, **3**, 85-130 (1952).

[2] W.P. Mason, Physical Acoustics and the Properties of Solids, D. Van Nostrand Co. Inc., (Princeton, New Jersey (19)

[3] IEEE Standard on Piezoelectricity (1987): [ANSI/IEEE Standard 176-1987]

[4] D.A. Berlincourt, D.R. Curran and H. Jaffe, Physical Acoustics I Part A: Chapter 3, pp.169-270, Academic Press, Editor: W.P. Mason.

[5] A.H. Meitzler, H.M. O'Bryan and H.F. Tiersten, *IEEE Trans.on Sonics and Ultrasonics*, **SU-20**, 233-239 (1973).

[6] R. Holland, *IEEE Trans. On Sonics and Ultrasonics*, **SU-14**, pp.18-20 (1967).

[7] S. Sherrit, Losses, Dispersion and Field Dependence of Piezoelectric Materials, Ph.D Thesis at Queen's University, Kingston, Ontario, Canada (January 1997).

[8] R. Holland and E.P.Eernisse, *IEEE Trans. On Sonics and Ultrasonics*, **SU-16 (4)**, pp.173-181 (1969).

[9] H. Ohigashi, T. Itoh, K. Kimura, T. Nakanishi and M. Suzuki, *Jap. J. Appl. Phys.*, **27**, pp.354-360 (1988).

[10] T. Tsurumi, T. Ichihara, K. Asaga and M. Daimon, *J. Amer. Cer. Soc.*, **73(5)**, pp.1330-1333 (1990).

[11] J.G. Smits, *IEEE Trans. Sonics and Ultrasonics*, **SU-23**, pp.393-402 (1976).

[12] S. Sherrit, H. D. Wiederick and B.K. Mukherjee, *Ferroelectrics*, **134**, pp.111-119 (1992).

[13] S. Sherrit, N. Gauthier, H.D. Wiederick and B.K. Mukherjee, *Ferroelectrics*, **119**, pp.17-32 (1991).

[14] C. Alemany, A.M. Gonsalez, L. Pardo, B. Jimenez, F. Carmona and J. Mendiola, *J. Phys. D: Appl. Phys.*, **28**, pp. 945-956 (1995).

[15] C.E. Land, G.W. Smith and C.R. Westgate, *IEEE Trans. On Sonics and Ultrasonics*, **SU-11**, pp.8-19 (1964).

[16] PRAP (Piezoelectric Resonance Analysis Programme) software available from TASI Technical Software, 174, Montreal Street, Kingston, Ontario K7K 3G4, Canada.

[17] S. Sherrit, H.D. Wiederick and B.K. Mukherjee, Medical Imaging 1997: Ultrasonic Transducer Engineering (SPIE Proceedings Volume 3037), pp.158-169 (1997).

[18] S. Sherrit, J.E. Haysom, H.D. Wiederick, B.K. Mukherjee and M. Sayer, Proc. Of the Tenth Int. Symp. On Applications of Ferroelectrics: ISAF'96, pp.959-962, IEEE, Piscataway, NJ, USA (1996).

[19] S. Butterworth, *Proc. Phys. Soc.*, **27**, pp.410-424 (1915).

[20] W. G. Cady, *Proc. IRE*, **10**, pp.83-114 (1922).

[21] S. Sherrit, H.D Wiederick, B.K. Mukherjee and M. Sayer, *J. Phys. D: Appl. Phys.*, **30**, pp.2354-2363 (1997).

[22] Q.M. Zhang, W.Y. Pan, S.J. Jang and L.E. Cross, *J. Appl. Phys.*, **64**, pp.6445-6451 (1988).

[23] H.D. Wiederick, S. Sherrit, R.B. Stimpson and B.K. Mukherjee, *Ferroelectrics*, **186**, pp.25-31 (1996).

[24] S. Sherrit, H.D. Wiederick, B.K. Mukherjee and M. Sayer, Smart Structures and Materials 1997: Smart Materials Technologies (SPIE Proceedings Volume 3040), pp.99-109 (1997), SPIE, Bellingham, Washington, USA.

[25] S. Sherrit, J.E. Haysom, H.D. Wiederick, B.K. Mukherjee and M. Sayer, Proc. Of the 10th Int. Symp.on Applications of Ferroelectrics: ISAF '96, pp.959-962, IEEE, Piscataway, NJ, USA (1996).

[26] S. Sherrit, R.B. Stimpson, H.D. Wiederick and B.K. Mukherjee, Smart Materials, Structures and MEMS (SPIE Proceedings Volume 3321), pp.74-81 (1996), SPIE, Bellingham, Washington, USA.

[27] S. Sherrit, D.B. Van Nice, J.T. Graham, B.K. Mukherjee and H.D. Wiederick, Proc. of the 8th Int. Symp. on Applications of Ferroelectrics: ISAF '92; pp. 167-170, IEEE, Piscataway, NJ, USA (1992).